Biochem. J. (2014) **459**, 193–203 (Printed in Great Britain) doi:10.1042/BJ20130558

Stability of the human pregnane X receptor is regulated by E3 ligase UBR5 and serine/threonine kinase DYRK2

Su Sien ONG*, Asli N. GOKTUG*, Ayesha ELIAS*, Jing WU*, Darren SAUNDERS† and Taosheng CHEN*[1]

*Department of Chemical Biology and Therapeutics, St. Jude Children's Research Hospital, 262 Danny Thomas Place, Memphis, TN 38105, U.S.A.
†Cancer Research Program, Garvan Institute of Medical Research, 384 Victoria Street, Darlinghurst NSW 2010, Australia

The hPXR (human pregnane X receptor), a major chemical toxin sensor, is a ligand-induced transcription factor activated by various xenobiotics and toxins, resulting in the transcriptional up-regulation of detoxifying enzymes. To date, little is known about the upstream regulation of hPXR. Using MS analysis and a kinome-wide siRNA screen, we report that the E3 ligase UBR5 (ubiquitin protein ligase E3 component n-recognin 5) and DYRK2 (dual-specificity tyrosine-phosphorylation-regulated kinase 2) regulate hPXR stability. UBR5 knockdown resulted in accumulation of cellular hPXR and a concomitant increase in hPXR activity, whereas the rescue of UBR5 knockdown decreased the cellular hPXR level and activity. Importantly, UBR5 exerted its effect in concert with the serine/threonine kinase DYRK2, as the knockdown of DYRK2 phenocopied UBR5 knockdown. hPXR was shown to be a substrate for DYRK2, and DYRK2-dependent phosphorylation of hPXR facilitated its subsequent ubiquitination by UBR5. This is the first report of the post-translational regulation of hPXR via phosphorylation-facilitated ubiquitination by DYRK2 and UBR5. The results of the present study reveal the role of the ubiquitin–proteasomal pathway in modulating hPXR activity and indicate that pharmacological inhibitors of the ubiquitin–proteasomal pathway that regulate hPXR stability may negatively affect treatment outcome from unintended hPXR-mediated drug–drug interactions.

Key words: dual-specificity tyrosine-phosphorylation-regulated kinase 2 (DYRK2), nuclear receptor, phosphorylation, pregnane X receptor (PXR), ubiquitination, ubiquitin protein ligase E3 component n-recognin 5 (UBR5).

INTRODUCTION

The human liver detoxification system comprises transporters and drug-metabolizing enzymes and is tightly governed by the hPXR [human PXR (pregnane X receptor)], a member of the nuclear receptor family [1]. hPXR has been shown to be activated by a wide array of compounds, both endogenous and exogenous, including bile acids, xenobiotics, herbal supplements and prescription medications [2–4]. Ligand-induced activation of hPXR leads to the transcriptional up-regulation of many drug-metabolizing enzymes and transporters, namely CYP3A4 (cytochrome P450 3A4) [5,6], the efflux pump protein MDR1 (multidrug resistance protein 1) [7] and UGT1A1 (UDP-glucuronosyl transferase 1A1) [8], which can lead to xenobiotic detoxification and pharmacoresistance. The ligand promiscuity of hPXR often leads to undesirable cross-reactivity with many prescription pharmaceuticals, prompting heavy investments in eliminating the PXR-activating effect of drug candidates. As a result, the downstream regulation of hPXR and its target genes is well characterized. However, little is known about the upstream regulation of hPXR, which can occur through the modulation of its protein level and activity. Some post-translational modifications of hPXR have been reported, such as phosphorylation [9] and more recently ubiquitination and SUMOylation [10,11].

Phosphorylation commonly occurs at tyrosine residues by tyrosine kinases or serine/threonine residues by serine/threonine kinases. Phosphorylation of hPXR mainly occurs at serine and threonine residues, and this phosphorylation is mainly associated with the negative regulation of its activity [12]. Experiments using phosphomimetic mutants further show that phosphorylation on hPXR alters its subcellular localization [13] or abrogates the recruitments of co-activators [14]. Ubiquitination is a process by which ubiquitin moieties are added on to lysine residues of a target protein. Ubiquitination is a multistep process involving the sequential transfer of a ubiquitin molecule between an E1 ubiquitin-activating enzyme, an E2 ubiquitin-conjugating enzyme and an E3 ubiquitin ligase [15]. Depending on how the ubiquitin moieties are attached, the target protein may have different fates, ranging from proteasomal-mediated degradation to relocalization into various cellular compartments [15]. In addition to phosphorylation, ubiquitination of hPXR further serves to modulate its activity. hPXR was shown to interact with SUG1 (suppressor for gal1), a component of the proteasome, in a progesterone-dependent manner to result in the degradation of PXR [16,17]. More recently, ubiquitination on hPXR has been reported and RBCK1 (RanBP-type and C3HC4-type zinc finger-containing 1) was identified as an E3 ligase responsible for ubiquitinating hPXR [10,11]. Thus post-translational modifications of nuclear receptors, including hPXR, contribute to regulating their activity and function. Understanding how hPXR is regulated is an important, yet less explored, avenue in modulating drug–drug interactions and drug resistance.

In the present study, we sought to identify other modulators of hPXR activity and function. We used a siRNA-based

Abbreviations: CA, catalytically inactive; CUL4A, cullin 4A; CYP3A4, cytochrome p450 3A4; DDB1, DNA damage-binding protein 1; DYRK2, dual-specificity tyrosine-phosphorylation-regulated kinase 2; fPXR, FLAG–hPXR; GAPDH, glyceraldehyde-3-phosphate dehydrogenase; HEK, human embryonic kidney; hPXR, human PXR; KD, kinase-dead; PXR, pregnane X receptor; RBCK1, RanBP-type and C3HC4-type zinc finger-containing 1; RbBP7, histone-binding protein 7; RT–PCR, reverse transcription PCR; SSMD, strictly standardized mean difference; SUG1, suppressor for gal1; TBS, Tris-buffered saline; UGT1A1, UDP-glucuronosyl transferase 1A1; VPRBP, Vpr (HIV-1)-binding protein; WT, wild-type.

[1] To whom correspondence should be addressed (email taosheng.chen@stjude.org).

screen of human kinases and MS analysis to show that the UBR5, in conjunction with DYRK2 (dual-specificity tyrosine-phosphorylation-regulated kinase 2), negatively regulates hPXR stability and activity. We show that hPXR can be phosphorylated by DYRK2 and this phosphorylation facilitates the ubiquitination of hPXR by UBR5. We further determined that DYRK2 and UBR5 exert their function as a multiprotein complex to regulate hPXR homoeostasis. The results of the present study provide the molecular mechanisms by which hPXR stability is regulated.

MATERIALS AND METHODS

Cell culture, plasmids and antibodies

HepG2 human liver carcinoma and HEK (human embryonic kidney)-293T cell lines were obtained from the A.T.C.C. (Manassas, VA, U.S.A.). Cells were grown in minimum essential medium or Dulbecco's modified Eagle's medium supplemented with 10 % FBS, 100 units/ml penicillin and 100 μg/ml streptomycin, 2 mM L-glutamine and 1 mM sodium pyruvate. Primary human hepatocytes were obtained through the Liver Tissue Cell Distribution System (donor 13-004) (Pittsburgh, PA, U.S.A.) or Triangle Research Laboratories (donors HUM4046 and GC4003) (Ashville, NC, U.S.A.). The primary hepatocytes were maintained in Williams' Medium E (Sigma–Aldrich) supplemented cell maintenance supplement (Life Technologies). HEK-293T cells stably expressing fPXR (FLAG–hPXR) were used to establish stable knockdown of UBR5, DYRK2 or a non-targeting control. Briefly, HEK-293T/fPXR cells were transduced with a shRNAs targeting the 3′-UTR of UBR5 (shUBR5) or the 3′-UTR of DYRK2 (shDYRK2), or non-targeting shRNA (NT). Non-targeting shRNA, shUBR5 and shDYRK2 were from Sigma–Aldrich and purchased as transfection-ready lentiviral particles. The knockdown of UBR5 or DYRK2 was confirmed by Western blot analysis. Cells were cultured in an incubator with a humidified atmosphere maintained at 5 % CO_2 and 37 °C. FLAG–DYRK2 [18] was purchased from Addgene. pcDNA3-FLAG-hPXR and *CYP3A4* luciferase reporter (CYP3A4-luc) plasmids were generated as described previously [19]. SF2-FLAG-hPXR was constructed by using standard molecular biology methods. The SF2 hybrid promoter uses the SFFVp (spleen focus-forming virus) LTR (long terminal repeat) enhancer fused to the CMV (cytomegalovirus) TATA box (provided by Dr John Gray). GFP-WT UBR5 and GFP-CA UBR5 (C2768A) were generated in the laboratory of Darren Saunders. The following antibodies were used: anti-GFP, anti-UBR5, anti-PXR (H-11; catalogue number sc-48340) and anti-ubiquitin (Santa Cruz Biotechnology); anti-DYRK2 (Abcam), anti-DDB1 (DNA damage-binding protein 1), anti-CUL4A (cullin 4A), anti-VPRBP [Vpr (HIV-1)-binding protein] and anti-RbBP7 (histone-binding protein 7) (Bethyl Laboratories); anti-GAPDH (glyceraldehyde-3-phosphate dehydrogenase; Ambion); and anti-FLAG (Sigma–Aldrich). The anti-CYP3A4 (K03) antibody was described previously [20].

Transient transfections, immunoprecipitation and immunoblotting

Transient transfections were performed using Lipofectamine™ 2000 (Invitrogen) according to the manufacturer's protocol. Cell lysates were prepared by using 0.5 % Triton X-100 lysis buffer [0.5 % Triton X-100, 20 mM Tris/HCl (pH 7.4), 5 mM EDTA and 150 mM NaCl] supplemented with 10 mM NaF, 10 mM sodium orthovanadate and Halt protease inhibitors (Pierce Biotechnology). Immunoprecipitation was performed on lysates by using 1 μg of specific antibodies conjugated to Protein A/G Plus beads (Santa Cruz Biotechnology) for 2 h at 4 °C. Immunoblotting was performed using standard protocols. One representative Western blot is shown for each study. The intensity of the protein band was quantified using LI-COR Odyssey software.

siRNA screen

The human kinome collection (Dharmacon) was reverse transfected into HepG2 cells stably expressing ectopic hPXR and CYP3A4-luc using Lipofectamine™ RNAiMAX (Life Technologies) at a final concentration of 25 nM. Briefly, reverse transfection is a process by which cells are overlaid on to a lipid/siRNA mix. Reverse transfection was employed since this process is more amenable to high-throughput assays. Cells were treated with rifampicin at a final concentration of 1.25 μM using pin-tool transfer at 72 h post-transfection. Luciferase readout was measured at 24 h post-rifampicin treatment. A robust SSMD (strictly standardized mean difference)-based algorithm on GUItars (a GUI tool for analysis of high-throughput RNA interference screening) was used for hit selection [21]. Briefly, SSMD is defined as the ratio of the mean to the S.D. of the random variable representing the difference between two independent populations. The bigger the magnitude of the SSMD between two populations is, the more the two populations are separate from each other. An siRNA with an SSMD $\geqslant$1 is considered a fairly moderate hit. In high-throughput assays, the data analysis methods should be robust to outliers. The robust version of SSMD (robust SSMD or SSMD*) can be obtained by replacing the mean with the median and S.D. with median absolute deviation [22]. The higher the SSMD score the higher possibility that the siRNA is a hit [23,24]. Putative negative regulators of hPXR activity were identified as having a robust SSMD value of $\geqslant$1. siDYRK2 was from Dharmacon, Qiagen and Novus Biologicals.

Luciferase assay

Cells either transiently transfected with CYP3A4-luc (the activity of CYP3A4-luc is regulated by hPXR and used to measure the transcription activity of hPXR) and TK-*Renilla* (used as a transfection control) plasmids or stably expressing the CYP3A4-luc plasmid were used to measure PXR activity, using rifampicin (Sigma–Aldrich) as the PXR agonist. Cells were plated on to 96-well plates in Phenol Red-free medium supplemented with 5 % charcoal-dextran-treated FBS. After 24 h, luciferase activity was measured by the SteadyLite Plus substrate (PerkinElmer) for cells stably expressing the CYP3A4-luc plasmid or the Dual-Glo substrate system (Promega) for transiently transfected cells. Luminescence was read on the EnVision plate reader (PerkinElmer). CYP3A4 promoter activity was expressed as the RLU (relative luciferase unit), which was determined by normalizing the firefly luciferase activity (from CYP3A4-luc) to the *Renilla* luciferase activity (from TK-*Renilla*) in the Dual-Glo assay, or represented by the total counts from the SteadyLite assay. The values represent the mean $\pm$ S.D. for three independent experiments.

RNA isolation and real-time RT–PCR

RNA was isolated using the Maxwell 16 LEV simplyRNA purification kit (Promega). Real-time RT–PCR (reverse transcription PCR) was used to measure the levels of mRNA, and was performed on Applied Biosystems 7900HT Fast Real-Time

PCR system (Life Technologies). Taqman probes were obtained from Life Technologies (catalogue number 4331182). Briefly, the cycle threshold (C_T) values of each gene of interest and of *GAPDH* were calculated for each sample, and then the normalized value was derived by subtracting the C_T value of GAPDH from that of the gene of interest (ΔC_T). Data are shown as mRNA fold change ($2^{-\Delta\Delta C_T}$) relative to the mRNA level of the corresponding transcript in the control samples as indicated. The values represent the means ± S.D. for three independent experiments.

MS analysis

HEK-293T cells were transiently transfected with pcDNA3.1 FLAG-PXR or pcDNA3.1-FLAG vectors using Lipofectamine™ 2000 according to the manufacturer's protocol. Cells were lysed with 1 % Triton X-100 lysis buffer [1 % Triton X-100, 20 mM Tris/HCl (pH 7.4), 5 mM EDTA and 150 mM NaCl] supplemented with 10 mM NaF, 10 mM sodium orthovanadate and Halt protease inhibitors. After centrifugation at 10000 ***g*** for 20 min, lysates were incubated with 10 μl of EZview Red anti-FLAG M2 affinity gel (Sigma–Aldrich) for 2 h at 4 °C. The M2 beads with the bound proteins were washed twice with the lysis buffer, twice with TBS (Tris-buffered saline), and eluted with 100 ng/μl FLAG peptide (Sigma–Aldrich) in TBS for 1 h at 4 °C. The eluted protein solution was mixed with ice-cold ethanol and incubated overnight at − 20 °C to precipitate the proteins. The solution was then centrifuged at 6000 ***g*** for 30 min and dried using a vacuum evaporator. The protein pellet was then submitted for processing and protein identification by the St. Jude Proteomics & Mass Spectrometry Shared Resource using an LTQ-Orbitrap mass spectrometer (ThermoFisher). Briefly, a solution phase digestion of the protein samples was performed using Lys-C and Trypsin. MS analysis was performed using an LTQ-Orbitrap mass spectrometer, which employs ESI (electrospray ionization), in conjunction with an Orbitrap mass analyser. The digest was introduced into the instrument via on line chromatography using reverse-phase (C_{18}) ultra-high pressure liquid chromatography using the nanoAcquity system (Waters). The column used was a Waters BEHC18 with an internal diameter of 75 μm and a bed length of 10 cm. The particle size was 1.7 μm. Peptides were gradient eluted into the linear ion trap through a non-coated spray needle with voltage applied to the liquid by increasing the concentration of acetonitrile. Data acquisition involved acquiring the peptide mass spectra followed by fragmentation of the peptide to produce MS/MS spectra that provides information about the peptide sequence. Protein/peptide assignments are made on the basis of the MS/MS spectra. The data were processed using the Mascot searching algorithm (Matrix Science) and Scaffold (Proteome Software) [25].

In vitro kinase assays

His–PXR (OriGene) immobilized on nickel beads (Qiagen) was used as a substrate. GST–WT (wild-type) DYRK2 (100 ng; SignalChem) was incubated with 1 μg of His–PXR or 1 μg of histone H1 (as a positive substrate control) in kinase buffer (25 mM Tris/HCl [pH 7.5], 5 mM 2-glycerophosphate, 2 mM DTT, 0.1 mM Na_3VO_4, 10 mM $MgCl_2$, 5 μM ATP and 10 μCi [γ-^{32}P]ATP) for 30 min at 30 °C. Reactions were terminated by adding SDS sample loading buffer followed by boiling the samples at 95 °C for 5 min. Samples were resolved by SDS/PAGE (4–12% gel), transferred on to PVDF membranes, and analysed by autoradiography or Western blotting.

In vitro ubiquitination assays

Reactions were carried out using 1 μg of purified His–PXR as the substrate in 50 μl of ubiquitination buffer containing 100 nM E1, 2.5 μM UbcH5a, 2.5 μM biotinylated ubiquitin, 5 mM Mg-ATP, and 1 mM DTT (ubiquitinylation kit; catalogue number BML-UW9920-0001; Enzo Life Sciences). GFP, GFP–WT UBR5 or GFP–CA (catalytically inactive) UBR5 immunoprecipitated by using an anti-GFP antibody from transiently transfected HEK-293T cells was used as a source of E3. The reaction mix was incubated for 90 min at 37 °C followed by three washes of RIPA lysis buffer.

Statistical analysis

Results are expressed as mean ± S.D. of at least three independent experiments. Student's *t* test was used to determine the statistical significance of the difference between the paired samples. For the grouped comparison in Figure 4(B), Kruskal–Wallis test was employed followed by Wilcoxon–Mann–Whitney post-hoc test for pairwise comparison. Differences were considered significant at $P < 0.05$ (signified by *).

RESULTS

DYRK2 negatively regulates hPXR activity

hPXR activity is known to be negatively regulated by phosphorylation [12]. To identify the kinases that regulate hPXR activity, we performed an siRNA screen against the human kinase collection using liver-derived HepG2 cells stably expressing ectopic hPXR and the CYP3A4 promoter luciferase plasmid (CYP3A4-luc); the activity of the CYP3A4 promoter is regulated by hPXR. As shown in the waterfall plot of Figure 1(A), the top hits identified as negative regulators of hPXR activity, including CDK4 (cyclin-dependent kinase 4), CDK18 (cyclin-dependent kinase 18) and DGKA (diacylglycerol kinase α) (denoted as dots on the waterfall plot; SSMD >1; see the Materials and methods section for more details), are involved in cell-cycle regulation and cellular proliferation, which is consistent with what we and other groups have reported previously [26,27]. Interestingly, DYRK2, which is involved in cell-cycle regulation and cellular growth, also emerged as one of the top hits from the screen (Figure 1A, inset, denoted with an X). DYRK2 was reported previously to be present in a complex containing the E3 ubiquitin protein ligase UBR5 and as mediating the stability of katanin [28].

To further confirm that DYRK2 is a negative regulator of hPXR activity, the activity of endogenous hPXR was measured in HepG2 cells stably expressing CYP3A4-luc against siRNA for DYRK2 (siDYRK2) obtained from different sources. This approach of measuring low expression levels of endogenous hPXR in HepG2 cells eliminates the possibility of an off-target effect of siRNA on the luciferase reporter gene. All siRNAs efficiently knocked down the DYRK2 transcript level (Supplementary Figure S1A http://www.biochemj.org/bj/459/bj4590193add.htm). Knockdown of DYRK2 consistently led to an increase in hPXR activity, as measured by luciferase readout (Figure 1B and Supplementary Figure S1C) and the endogenous CYP3A4 transcript level (Figure 1C and Supplementary Figure S1A). The increase in hPXR activity was not accompanied by an increase in the hPXR transcript level (Supplementary Figure S1A), ruling out the possibility of transcriptional regulation of hPXR. These results indicate that DYRK2 negatively regulates hPXR, most probably at a post-translational level.

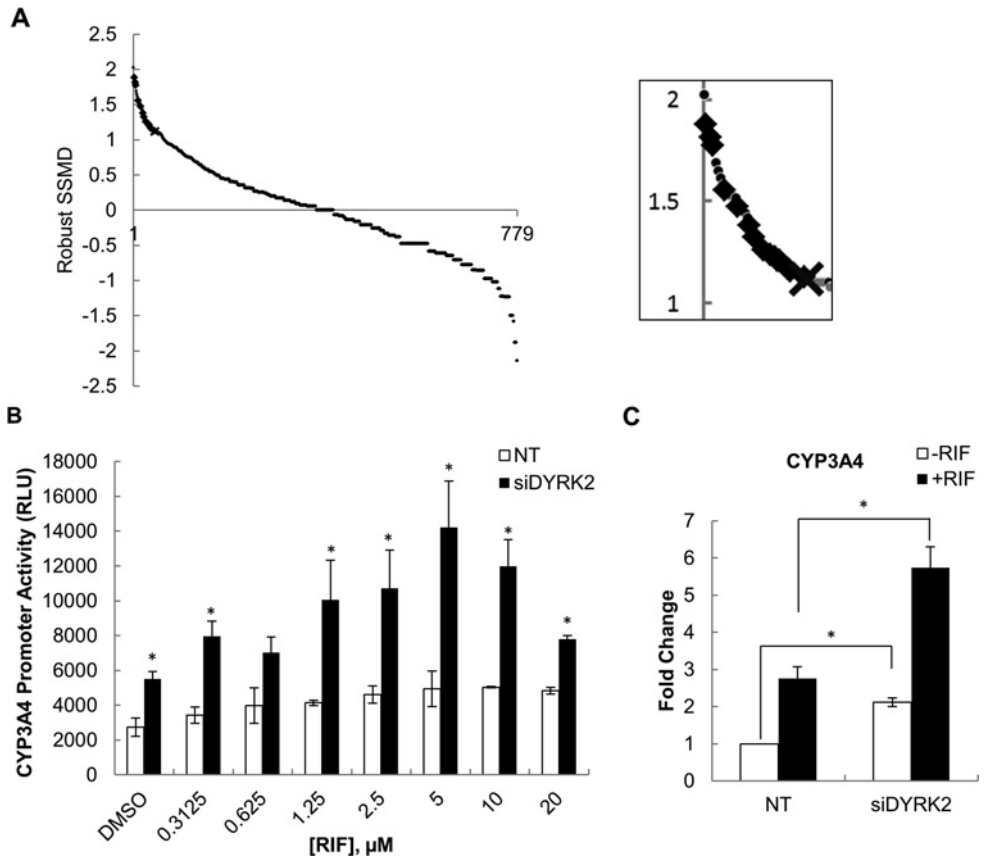

Figure 1 DYRK2 is a negative regulator of hPXR activity

(**A**) Waterfall plot of hits generated from a kinome-wide siRNA screen performed on HepG2 cells stably expressing hPXR and CYP3A4 promoter-driven luciferase plasmid (CYP3A4-luc). The *y*-axis displays the value of robust SSMD for each siRNA. Robust SSMD is a parameter used to select hit (see the Materials and methods section). Inset: magnified view of the waterfall plot showing DYRK2 (denoted with an X) as one of the top hits (robust SSMD >1). Cell-cycle regulated genes (◆) were found to be the top hits. (**B**) Rifampicin (RIF) dose–response of endogenous PXR activity following a non-targeting (NT) or DYRK2 knockdown (siDYRK2) in HepG2 cells stably expressing CYP3A4-luc. *$P < 0.05$, siDYRK2 compared with non-targeting siRNA. (**C**) RT–PCR of endogenous *CYP3A4* transcript level after non-targeting siRNA or siDYRK2 knockdown. The value from untreated (− RIF) non-targeting siRNA was set as 1. *$P < 0.05$, siDYRK2 compared with non-targeting siRNA.

hPXR associates with DYRK2 in a complex

The identification of DYRK2 as a negative regulator of hPXR, and the previous report that DYRK2 associated with UBR5 in a complex to regulate the stability of katanin [28], prompted us to determine whether hPXR interacts with DYRK2 and UBR5 in a multiprotein complex. To identify the binding partners of hPXR, HEK-293T cells transiently transfected with either an empty vector containing the FLAG epitope (as a negative control to eliminate non-specific-binding proteins) or fPXR were immunoprecipitated using M2–agarose beads and then analysed by MS. HEK-293T cells were chosen because they were used in the study that identified the interaction between DYRK2 and UBR5 [28]. HEK-293T cells do not express hPXR endogenously. UBR5, DDB1 and RbBP7 were among the putative binding partners identified (Figure 2A). UBR5 is a HECT (homologous with E6-associated protein C-terminus) domain-containing E3 ligase that targets proteins for proteasomal-mediated degradation. DDB1 functions in nucleotide excision repair and is also a component of the CUL4–X-box E3 ligase complex. DDB1 is also found in a complex containing UBR5 [28]. RbBP7 is a WD40 domain-containing protein also found in a complex with the DDB1–CUL4A complex [29]. To confirm the results from the MS analysis, we transiently overexpressed FLAG or fPXR in HEK-293T cells and performed co-immunoprecipitation assays. UBR5 interacted with hPXR in cells, and Western blot analysis indicated that this interaction occurs in a complex containing DDB1 and RbBP7, as suggested by the data obtained from the MS analysis (Figure 2B). DYRK2 was also detected in this complex (Figure 2B), although it was not identified from the MS analysis. Since VPRBP1 is the substrate-recognition component of the E3 ligase complex containing UBR5 and DDB1, as reported by Maddika and Chen [28], we checked whether VPRBP1 was present in this complex. We found that VPRBP1 was not an interacting protein (Figure 2B). Since both VPRBP1 and RBBP7 contain WD40 domains, we reasoned that RBBP7 may be the substrate-recognition protein that recruits PXR to the complex. CUL4A was also not detected in this complex, which precludes the possibility that hPXR interacted with RBBP7 in a complex containing CUL4A. Taken together, these results indicate that hPXR associates with DYRK2 in a multiprotein complex that also contains UBR5, DDB1 and RBBP7, and suggest that UBR5 might contribute to the negative regulation of hPXR by DYRK2.

hPXR is ubiquitinated

Because hPXR occurred in a complex that contained the E3 ubiquitin ligase UBR5, we investigated whether hPXR was degraded through the ubiquitin–proteasomal pathway. Protein levels of hPXR increased by 60 % in HEK-293T cells stably

A

Interacting Protein	No. of unique peptides	
	Flag	Flag-PXR
Histone-binding protein (RbBP7)	0	2
DNA damage binding protein 1 (DDB1)	0	2
E3 ubiquitin-protein ligase 5 (UBR5)	0	2

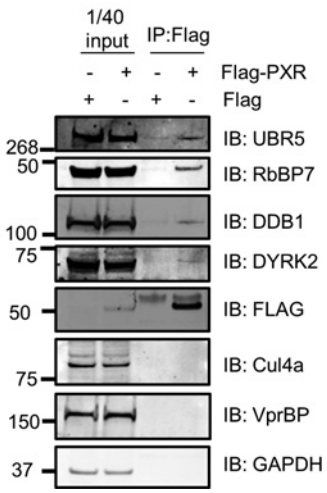

Figure 2 hPXR interacts with DYRK2 in a multiprotein complex containing UBR5

(**A**) hPXR-associated proteins and the corresponding number of peptides identified using MS analysis. (**B**) Co-immunoprecipitation using anti-FLAG antibodies (IP: FLAG) in HEK-293T cells expressing fPXR to confirm the presence of the associated proteins identified by MS. The association was confirmed by antibodies against UBR5, DDB1, DYRK2 and RbBP7 using Western blot analysis (IB). 1/40 input indicates 2.5 % of the input lysates were used to show the expression level of the proteins. GAPDH was used as a loading control. Molecular mass markers are indicated on the left-hand side.

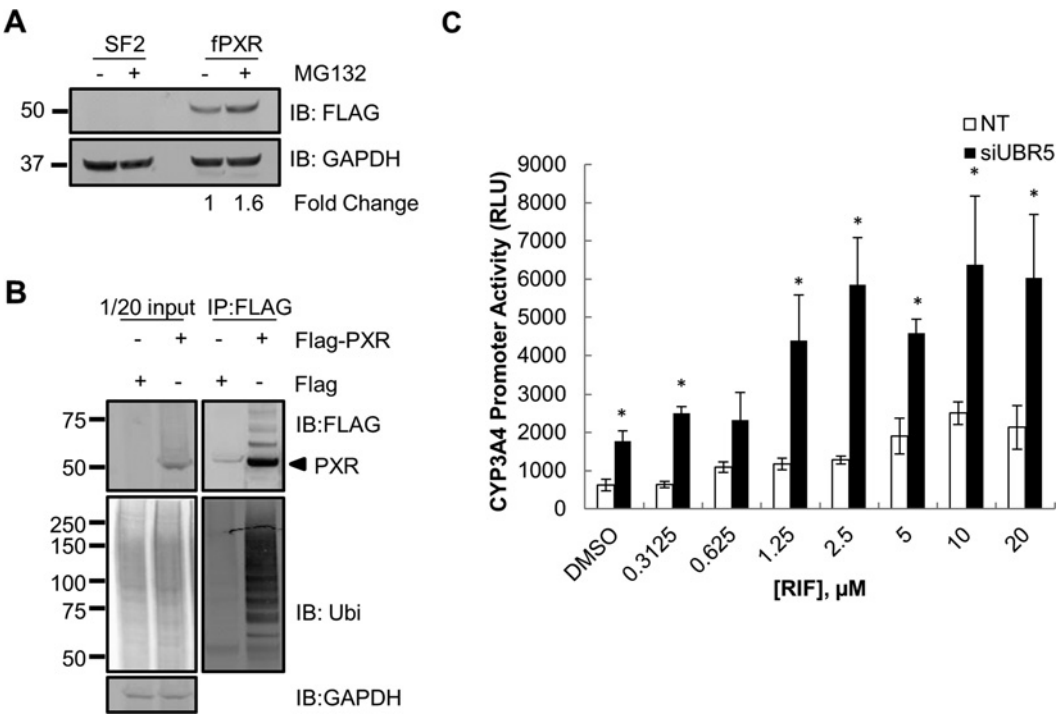

Figure 3 hPXR undergoes UBR5-dependent polyubiquitination

(**A**) HEK-293T cells stably expressing fPXR were treated either with the vehicle control DMSO (−) or 10 μM MG132 (+) for 6 h followed by Western blotting analysis to determine the cellular hPXR level. SF2, empty vector control. The numbers at the bottom indicate the relative fold change in the fPXR bands, with the DMSO-treated sample set as 1. (**B**) HEK-293T cells stably expressing fPXR or an empty vector control (Flag) were treated either with the vehicle control DMSO (−) or 10 μM MG132 (+) for 6 h followed by immunoprecipitation (IP) using an anti-FLAG antibody and Western blotting analysis using antibodies against ubiquitin (Ubi) and the FLAG epitope. 1/20 input indicates 5 % of the input lysates were used to show the expression level of the proteins. (**C**) Knockdown of UBR5 (siUBR5) was performed in HepG2 cells stably expressing CYP3A4-luc. At 72 h post-transfection with either siUBR5 or the non-targeting (NT) control, the transfected cells were treated with either RIF or DMSO as indicated. CYP3A4-luc activity was measured at 24 h post-RIF or -DMSO treatment. Molecular mass markers are indicated on the left-hand side of the Western blot images. *$P < 0.05$ siUBR5 compared with non-targeting control. IB, immunoblot.

expressing fPXR treated with the proteasomal inhibitor MG132 (Figure 3A, right-hand lanes), suggesting that hPXR is a substrate for the proteasome. To determine whether hPXR was ubiquitinated, we immunoprecipitated fPXR from the MG132-treated cells by using an anti-FLAG antibody, followed by Western blotting analysis using antibodies against the FLAG epitope (Figure 3B, top panel) or ubiquitin (Figure 3B, middle panel). hPXR underwent significant ubiquitination (Figure 3B),

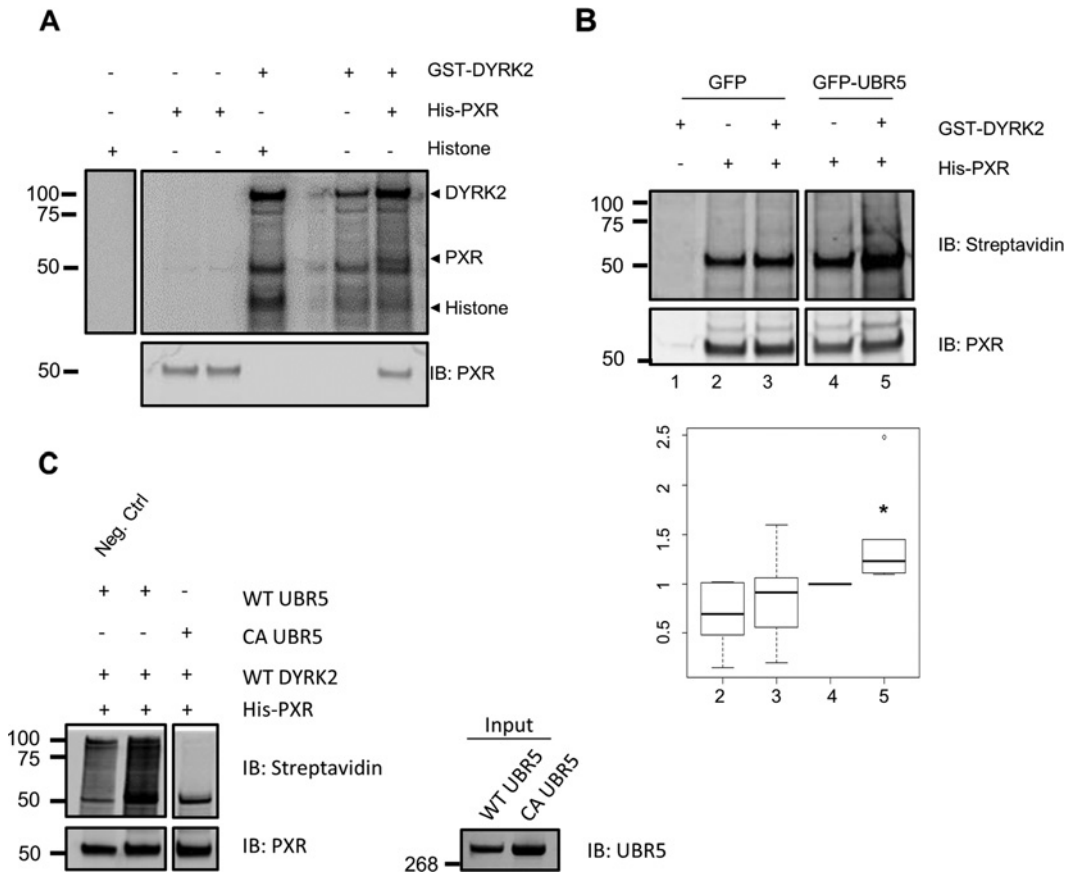

Figure 4 hPXR is a substrate for DYRK2 and UBR5

(**A**) *In vitro* kinase assay using purified GST–WT DYRK2 (DYRK2) and His-tagged hPXR (His–PXR). Histone was used as a positive control for the kinase activity of DYRK2. (**B**) *In vitro* ubiquitination assay using purified His–PXR in the presence of GFP (as a negative control) or GFP–WT UBR5 (GFP-UBR5) as a source of E3 ligase. Ubiquitinated His–hPXR was detected using streptavidin, which recognizes biotinylated ubiquitin. The histogram shows the average relative intensity of the area representing the ubiquitinated hPXR from three independent experiments. $*P < 0.05$ (for grouped comparison among lanes 2, 3, 4 and 5, Kruskal–Wallis test was employed, followed by Wilcoxon–Mann–Whitney post-hoc test for pairwise comparison). Lanes 1–5 are all from the same gel. (**C**) Left-hand panel: *in vitro* ubiquitination assay using purified His–hPXR in the presence of either GFP–WT UBR5 or GFP–CA UBR5 as a source of E3 ligase. Neg. Crtl, EDTA was added to the sample to inhibit the reaction process and serves as a negative control. The amounts of input His–PXR are shown in the lower panel, as revealed in a paralleled Western blotting analysis using anti-PXR antibodies. Right-hand panel: Western blotting analysis showing the amount of WT UBR5 and CA UBR5 used in the *in vitro* ubiquitination reaction. Molecular mass markers are indicated on the left-hand side of the Western blot images. IB, immunoblot.

as evidenced by the higher-molecular-mass laddering of hPXR (Figure 3B, top panel, right-hand lane) and the corresponding ubiquitin immunoblot (Figure 3B, middle panel, right-hand lane). These results indicated that hPXR is ubiquitinated and degraded through the ubiquitin–proteasomal pathway. Next, we sought to determine whether UBR5 also functions as a negative regulator of hPXR activity. We used HepG2 stably expressing the CYP3A4-luc, the same cellular model in which we demonstrated DYRK2 as a negative regulator of hPXR activity (Figure 1B). As shown in Figure 3(C), knockdown of UBR5 using siRNA against UBR5 (siUBR5) led to higher activity of hPXR, as revealed by the increased activity of the hPXR-regulated CYP3A4 promoter. These results indicate that UBR5 is a negative regulator of hPXR.

hPXR is a substrate for DYRK2 and UBR5

We then sought to determine whether hPXR is a substrate for DYRK2 and UBR5, and whether DYRK2 exerts its function by phosphorylating hPXR and facilitating its ubiquitination by UBR5. In an *in vitro* kinase assay we demonstrated that purified WT DYRK2 phosphorylates purified hPXR (Figure 4A, upper panel, right-hand lane), indicating that hPXR is a substrate for DYRK2. Histone H1 was used as a positive substrate control in the assays (Figure 4A, upper panel). Next, we tested whether PXR was the substrate for UBR5 *in vitro*. We used GFP–UBR5 or GFP, transiently expressed and immunoprecipitated from HEK-293T cells, as a source of E3 or a negative control respectively. As shown in Figure 4(B), in the *in vitro* ubiquitination assay GFP–UBR5, but not GFP, mediated the ubiquitination of purified His–PXR in the presence of purified DYRK2. As an additional negative control, we showed that a CA UBR5 failed to mediate hPXR ubiquitination (Figure 4C, left-hand panels). Taken together, these results indicate that hPXR is a substrate for DYRK2 and UBR5, and the kinase activity of DYRK2 facilitates the efficient ubiquitination of hPXR.

UBR5 and DYRK2 regulate the protein level and activity of hPXR

To further study the effect of UBR5 and DYRK2 on hPXR, we determined whether modulation of the cellular levels of UBR5 and DYRK2 affected the ubiquitination status, protein level and activity of hPXR.

We first transiently knocked down UBR5 in HEK-293T cells stably expressing either FLAG vector (SF2) or fPXR. Transient

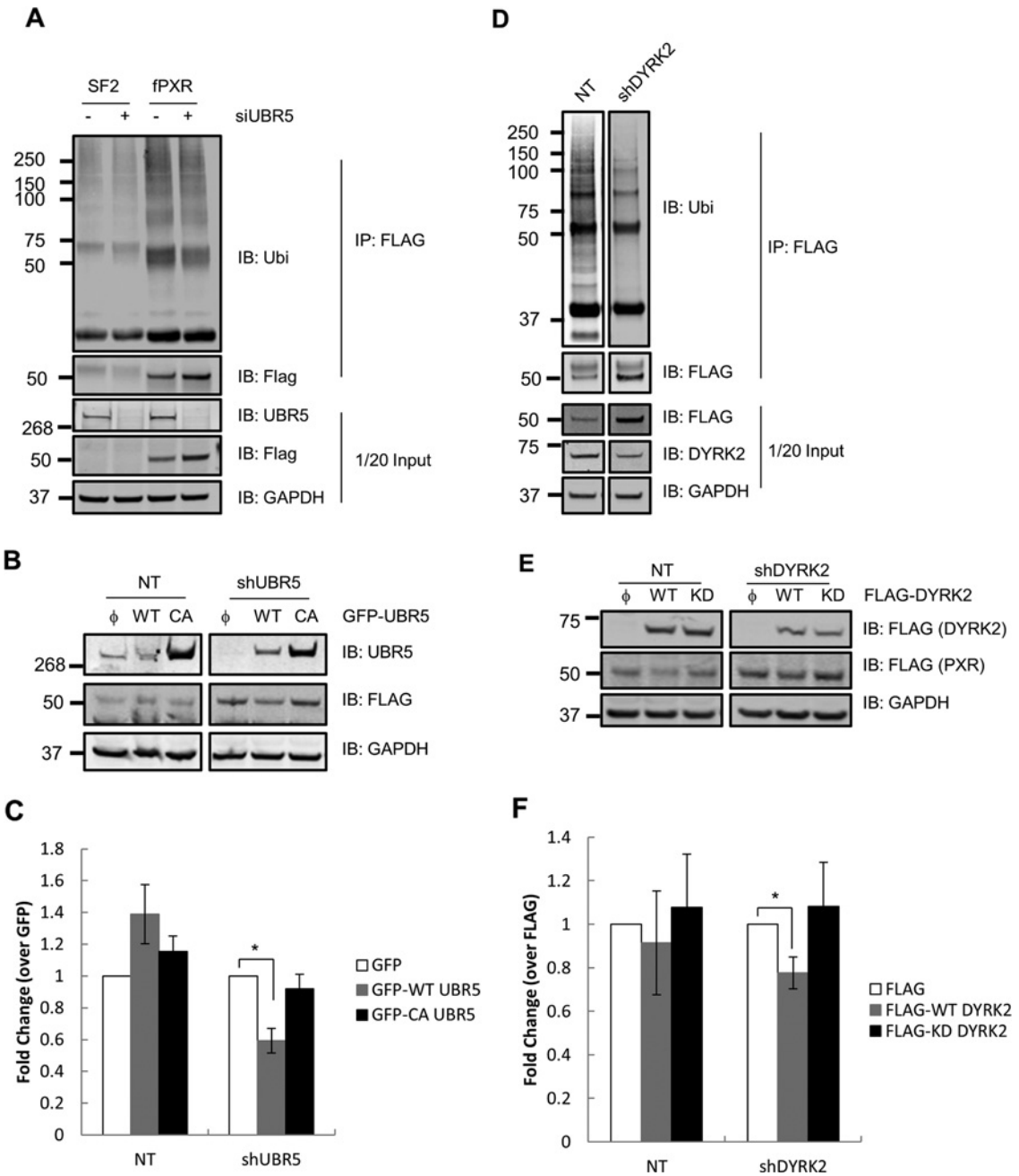

Figure 5 hPXR level is modulated by UBR5 and DYRK2

(**A**) siRNA knockdown of UBR5 (+ siUBR5) or non-targeting control (−) was performed on HEK-293T cells stably expressing an empty vector (SF2) or SF2-FLAG-hPXR (fPXR). At 72 h post-transfection, the cells were treated with 10 μM MG132 for 6 h, followed by an immunoprecipitation using an anti-FLAG antibody and immunoblotting using antibodies as indicated. (**B**) A stable knockdown of UBR5 was performed on HEK-293T cells stably expressing fPXR using shRNA targeting the 3′-UTR of UBR5 (shUBR5). A rescue experiment was done by transiently overexpressing knockdown-resistant WT UBR5 (WT) or CA UBR5 (CA). Total hPXR was determined using an antibody against the FLAG epitope. (**C**) Quantification of (**B**) by normalizing the hPXR level to the *GAPDH* level. $*P < 0.05$, for results from at least three independent experiments. (**D**) Stable knockdown of DYRK2 on HEK-293T cells stably expressing fPXR was performed using shRNA against the 3′-UTR of DYRK2 (shDYRK2). fPXR was immunoprecipitated from cells pre-treated with 10 μM MG132 for 6 h. Ubiquitinated hPXR was visualized using an antibody against ubiquitin. (**E**) Rescue experiment was performed by transiently overexpressing knockdown-resistant WT DYRK2 (WT) or KD DYRK2 (KD). Total hPXR level was determined using an antibody against the FLAG epitope. (**F**) Quantification of (**E**) by normalizing the hPXR level to the *GAPDH* level. $*P < 0.05$, for results from at least three independent experiments. Molecular mass markers are indicated on the left-hand side of the Western blot images. Φ, empty vector control; IB, immunoblot; IP, immunoprecipitation; NT, non-targeting shRNA control; Ubi, ubiquitin.

UBR5 knockdown led to a decrease in hPXR ubiquitination (Figure 5A, top panel, right-hand lanes) and a concomitant increase in hPXR protein level (Figure 5A, second panel from top, right-hand lanes). This increase in protein level was not accompanied by an increase in the hPXR transcript level (results not shown). To further show that the increase in cellular level of hPXR is mediated through the knockdown of UBR5, we used HEK-293T/fPXR cells to stably and efficiently knock down UBR5 by using a shRNA against UBR5 (shUBR5) that targets the 3′-UTR of UBR5; non-targeting shRNA (NT) was used in

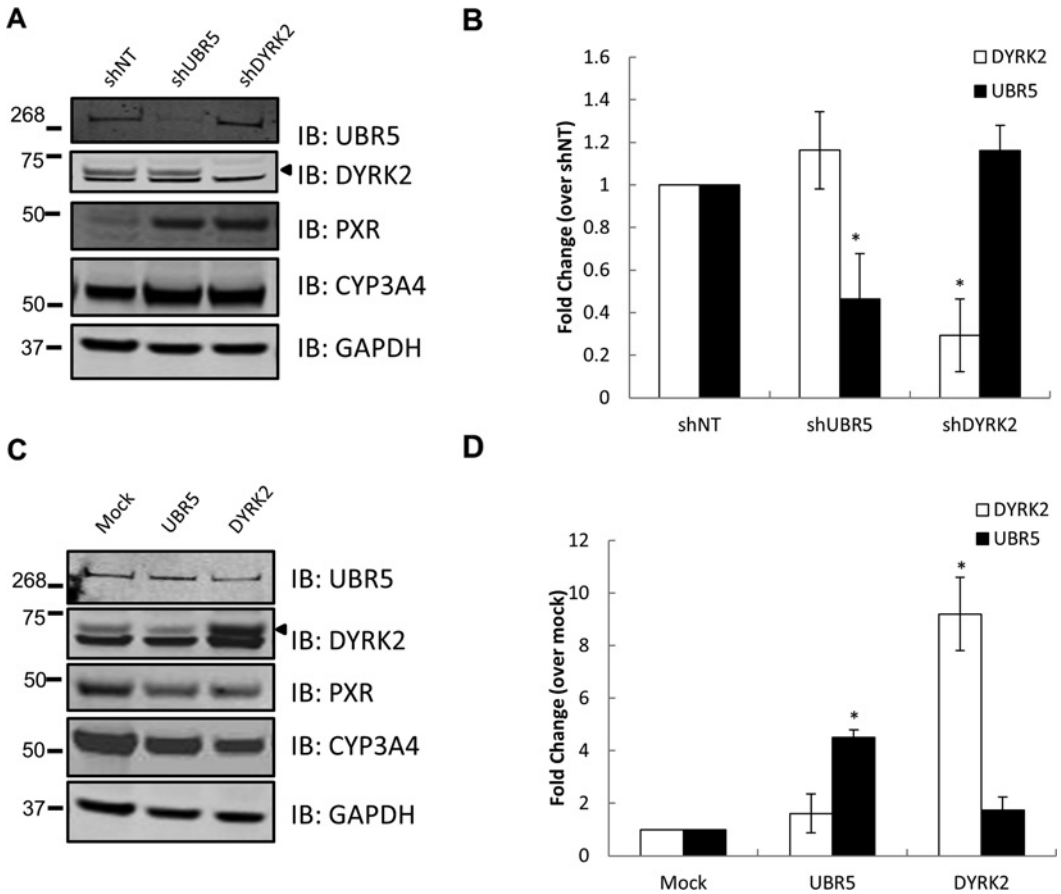

Figure 6 hPXR level and activity are modulated by UBR5 and DYRK2 in human primary hepatocytes

(**A**) shRNA knockdown of UBR5 (shUBR5) and DYRK2 (shDYRK2) was performed on primary hepatocytes. At 72 h post-transduction, the cells were harvested and subjected to Western blot analysis using the antibodies indicated. The images show results from one donor (HUM4046). (**B**) RT–PCR of the samples in (**A**) using probes specific to UBR5 and DYRK2. The value from the non-targeting shRNA (shNT) was set as 1. Student's *t* test was used to determine the statistical significance of the difference between shUBR5 or shDYRK2 and the non-targeting shRNA (**B**), and DYRK2 or UBR5 and a mock-transfected sample (**D**). $*P < 0.05$, of results from three different donors. (**C**) Transient overexpression of UBR5 or DYRK2 into primary hepatocytes followed by Western blotting analysis at 48 h post-transfection. (**D**) RT–PCR of the samples in (**C**) using probes specific to UBR5 and DYRK2. The value from mock transfection was set as 1. Arrow heads in (**A**) and (**C**) indicate DYRK2. Molecular mass markers are indicated on the left-hand side of the Western blot images. IB, immunoblot.

control cells (Figure 5B, top panel, Φ). Stable knockdown of UBR5 increased the protein level of hPXR (Figure 5B, middle panel, Φ), which was partially rescued by reintroducing WT UBR5, but not CA UBR5 (neither plasmid contains a 3′-UTR of UBR5 so they are insensitive to the regulation of shUBR5) (Figure 5B, shUBR5). Figure 5(C) shows the quantified levels of hPXR observed in Figure 5(B). These results indicate that the level of hPXR is inversely correlated with those of WT UBR5.

Since DYRK2 and UBR5 exerted their functions on hPXR in a complex, we next determined whether modulation of DYRK2 had the same effect as UBR5 modulation. Stable knockdown of DYRK2 using shDYRK2 that targets the 3′-UTR of DYRK2 in HEK-293T/fPXR cells led to an increase in the protein level of hPXR and a concomitant decrease in hPXR ubiquitination (Figure 5D). Importantly, the level of hPXR ubiquitination (Figure 5D, top panel) was inversely correlated with the total hPXR level (Figure 5D, second panel from top). To determine whether the change in hPXR was dependent on the DYRK2 level, a rescue experiment was performed in this stable knockdown cell system. The HEK-293T/fPXR cells stably expressing shRNA against the 3′-UTR of DYRK2 were transiently transfected with WT DYRK2 or the KD (kinase-dead) mutant of DYRK2. The increase in hPXR protein level was partially rescued by the reintroduction of WT DYRK2, but not KD DYRK2, confirming that the kinase activity of DYRK2 is required for its function (Figure 5E). Figure 5(F) shows the quantified levels of hPXR observed in Figure 5(E). These results indicate that the level of hPXR is inversely correlated with those of WT DYRK2.

To further confirm our observations, we examined the effect of knocking down or overexpressing UBR5 or DYRK2 on the level and activity of PXR in primary human hepatocytes. As shown in Figures 6(A) and 6(B), shRNA against UBR5 and DYRK2 knocked down UBR5 and DYRK2 respectively, which was accompanied by a concomitant increase in the hPXR protein level. Conversely, the ectopic expression of DYRK2 and UBR5 led to a decrease in hPXR protein level (Figures 6C and 6D). Importantly, modulation of hPXR protein levels led to corresponding changes in CYP3A4 protein levels.

To further determine the effect of reintroducing UBR5 and DYRK2 on the activity of hPXR, we used HEK-293T/fPXR cells stably expressing either shUBR5 or shDYRK2 and transfected with CYP3A4-luc. Reintroduction of WT UBR5, but not CA UBR5 or empty vector (GFP), to HEK-293T/fPXR/shUBR5 cells led to a decrease in PXR activity (Figure 7A). Similarly, reintroduction of WT DYRK2, but not KD DYRK2 or empty vector (FLAG), to HEK-293T/fPXR/shDYRK2 cells led to a

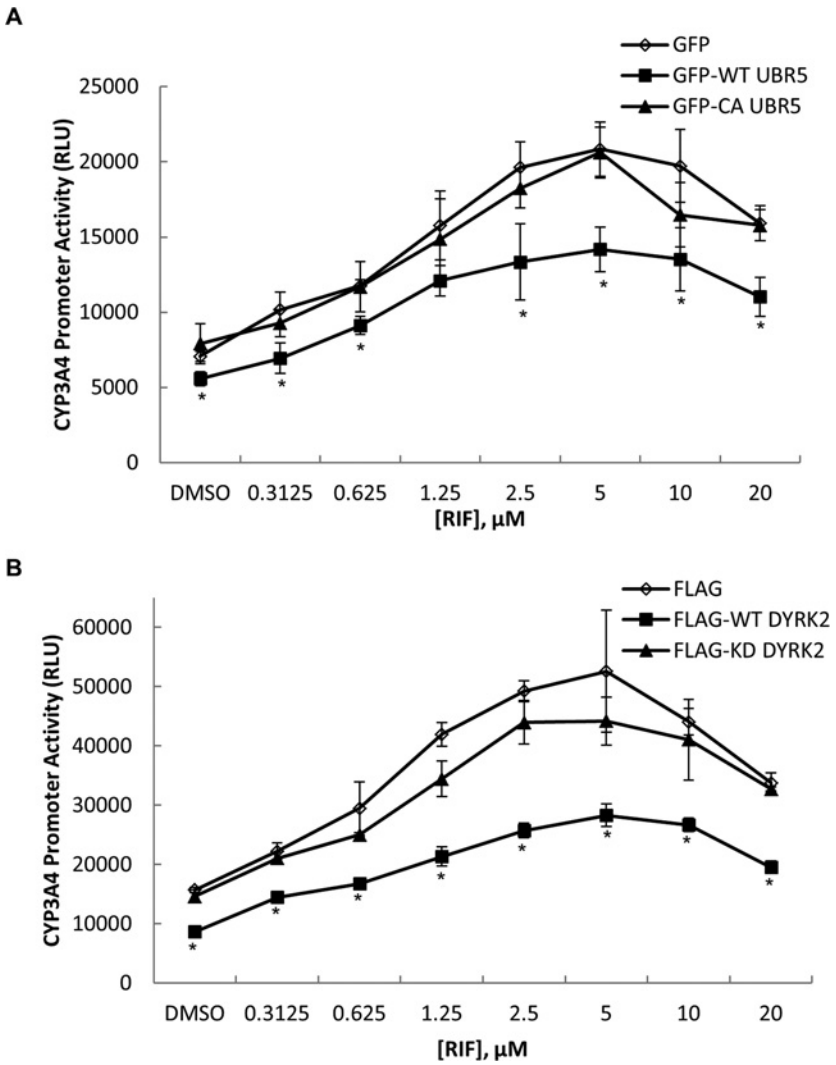

Figure 7 hPXR activity is modulated by UBR5 and DYRK2

(**A**) GFP vector (GFP), GFP-tagged WT UBR5 (GFP-WT UBR5) or CA UBR5 was reconstituted into HEK-293T cells stably expressing shRNA against the 3′-UTR of UBR5. hPXR activity was measured by luciferase-based CYP3A4 promoter activity following treatment with DMSO or a dose–response of rifampicin (RIF) for 24 h. (**B**) FLAG vector (FLAG), FLAG-tagged WT DYRK2 or KD DYRK2 were reconstituted into HEK-293T cells stably expressing shRNA against the 3′-UTR of DYRK2. hPXR activity was measured by luciferase-based CYP3A4 promoter activity following treatment with DMSO or a dose–response of rifampicin for 24 h. $^*P < 0.05$.

decrease in PXR activity (Figure 7B). Taken together, the results of the present study indicate that UBR5 and DYRK2 play a role in regulating hPXR protein level and activity.

DISCUSSION

hPXR is a master transcriptional regulator of xenobiotic detoxification enzymes that is predominantly expressed in the liver and intestines. In the resting state, hPXR is transcriptionally repressed by binding to co-repressors [30]. Ligand binding to hPXR leads to the dissociation of co-repressors and the recruitment of co-activators, resulting in a transcriptionally active hPXR. Surprisingly, we observed that the increase in cellular hPXR level can increase its basal activity, seemingly independent of ligand engagement. Since we cannot preclude the possibility of the presence of endogenous ligands of hPXR in our experimental model, and because of the ligand promiscuity of hPXR, elevated levels of hPXR may enhance the effect of low-potency hPXR agonists. Our findings suggest that an increase in the cellular hPXR level is sufficient to induce transcriptional activation of its target genes. A positive correlation between hPXR level and its target gene levels has been seen in colorectal cancer [31]. An increase in hPXR level was observed with the decrease in chemosensitivity of irinotecan due to inactivation of the drug and its active metabolite SN-38 by CYP3A4-mediated oxidation and UGT1A1-mediated glucuronidation respectively [31]. hPXR can also form a transcriptionally active homodimer [32], which may explain the increase in basal hPXR activity in the absence of ligand. The increase in hPXR level (2-fold increase following MG132 treatment) is relatively modest in the present study, suggesting that hPXR stability may be governed by other factors. Indeed, PXR stability has been shown to be modulated via the ubiquitin–proteasomal system. In a yeast two-hybrid protein interaction assay, Masuyama et al. [16] showed that PXR interacts with SUG1, a component of the proteasome, in a progesterone-dependent manner. Interestingly, progesterone enhanced PXR degradation and overexpression of SUG1 led to proteolytic

PXR fragments, which was blocked by a proteasome inhibitor [16,17]. These data provided the first evidence that PXR may be degraded through a proteasome-mediated pathway. More recently, in another yeast two-hybrid screen, Rana et al. [10] identified the E3 ubiquitin ligase RBCK1 as an interacting partner of hPXR. They further demonstrated that RBCK1 ubiquitinates hPXR, thus targeting hPXR for degradation by the ubiquitin–proteasome pathways. The present study, by using MS analysis and a kinome-wide siRNA screen, identified a pathway that regulates hPXR stability via phosphorylation-facilitated ubiquitination by serine/threonine kinase DYRK2 and the E3 ubiquitin ligase UBR5, further confirming the role of the ubiquitin–proteasomal pathway in modulating hPXR levels. Since multiple E3 ligases can act on the same substrate, it is possible that hPXR is a substrate for multiple E3 ligases.

In the present study, we found that the E3 ligase UBR5 works in concert with the serine/threonine kinase DYRK2, possibly in a complex containing the adaptor proteins DDB1 and RbBP7, to mediate hPXR stability. UBR5, DYRK2, DDB1 and VPRBP were reported previously to be in a multiprotein complex that regulates the stability of katanin, where VPRBP serves as a substrate-recognition protein for katanin [28]. However, the substrate-recognition adaptor in the present study appears to be RbBP7 and not VPRBP. Since both RbBP7 and VPRBP contain WD40 domains, which is one of the most abundant domains in eukaryotes [33], it is exciting to speculate that the WD40 domain-containing adaptors confer substrate specificity to the UBR5–DYRK2 complex. Although our findings do not preclude the existence of other WD40 domain-containing proteins in the UBR5–DYRK2–DDB1 complex, they suggest that RbBP7 may act as the substrate-recognition component that recruits hPXR to the complex. We further showed that the kinase activity of DYRK2 is needed for its effect on facilitating UBR5-mediated ubiquitination of hPXR. However, we cannot rule out the role of DYRK2 as a scaffold in the multiprotein complex. Both the kinase activity and the scaffold function of DYRK2 are needed for the UBR5–DYRK2 complex to regulate the stability of katanin [28]. It is possible that DYRK2 is acting in the same manner here in exerting its function on hPXR. Further efforts to delineate the residues of hPXR that are phosphorylated by DYRK2 would be of interest. It is noteworthy that hPXR contains a consensus phosphorylation site for DYRK2 [34]. It is possible that the phosphorylation of this residue abrogates the ligand-binding capacity of hPXR.

In the experiments using primary hepatocytes, we noticed that the endogenous levels of UBR5 and DYRK2 were low. It is important to note that UBR5 expression[2] and DYRK2 expression[3] are down-regulated in the liver (shown in the present study by comparing the mRNA levels of *UBR5* and *DYRK2* in the human liver to those in other human tissues), whereas the hPXR level is highest in the liver, further suggesting an interplay among UBR5, DYRK2 and hPXR.

Since UBR5 [35,36] and DYRK2 [37,38] are often overexpressed in cancers, they are potential therapeutic targets. However, caution must be exercised while modulating UBR5 and DYRK2 at the hPXR protein level due to the possible resulting undesired drug–drug interactions and drug resistance. Future efforts in eliminating the PXR-activating effect of drug candidates in drug development should focus not only on determining whether the drug candidates bind to PXR, but also on studying how they affect the protein stability of PXR, since both factors affect the net activity of PXR and can cause adverse drug effects.

AUTHOR CONTRIBUTION

Asli Goktug participated in the siRNA screen and data analysis. Ayesha Elias performed the MS experiments. Jing Wu constructed and tested SF2-FLAG-hPXR. Darren Saunders generated and tested GFP–WT UBR5 and GFP–CA UBR5. Su Sien Ong performed all the other experiments. Su Sien Ong and Taosheng Chen designed the experiments, analysed the data and wrote the paper.

ACKNOWLEDGEMENTS

We thank Dr Vani Shanker (St. Jude Children's Research Hospital) for editing the paper before submission, Dr John Gray (St. Jude Children's Research Hospital) for providing the SF2 expression vector, the St. Jude Vector Core Laboratory and the St. Jude Proteomics & Mass Spectrometry Shared Resource for technical assistance, Ta Zhi Ong for assistance with statistical analysis, Yueming Wang and other members of the Chen Research Laboratory for valuable discussions. Normal human hepatocytes were obtained through the Liver Tissue Cell Distribution System (Pittsburgh, PA, U.S.A.), which was funded by NIH (National Institutes of Health) contract number N01-DK-7-0004/HHSN267200700004C.

FUNDING

This work was supported, in part, by the American Lebanese Syrian Associated Charities (ALSAC), St. Jude Children's Research Hospital, the National Institutes of Health National Institute of General Medical Sciences [grant number GM086415 (to T.C.)] and the National Institutes of Health National Cancer Institute [grant number P30-CA21765].

REFERENCES

1 Wang, Y. M., Ong, S. S., Chai, S. C. and Chen, T. (2012) Role of CAR and PXR in xenobiotic sensing and metabolism. Expert Opin. Drug Metab. Toxicol. **8**, 803–817
2 Kliewer, S. A. (2003) The nuclear pregnane X receptor regulates xenobiotic detoxification. J. Nutr. **133**, 2444S–2447S
3 Moore, L. B., Goodwin, B., Jones, S. A., Wisely, G. B., Serabjit-Singh, C. J., Willson, T. M., Collins, J. L. and Kliewer, S. A. (2000) St. John's wort induces hepatic drug metabolism through activation of the pregnane X receptor. Proc. Natl. Acad. Sci. U.S.A. **97**, 7500–7502
4 Xie, W., Radominska-Pandya, A., Shi, Y., Simon, C. M., Nelson, M. C., Ong, E. S., Waxman, D. J. and Evans, R. M. (2001) An essential role for nuclear receptors SXR/PXR in detoxification of cholestatic bile acids. Proc. Natl. Acad. Sci. U.S.A. **98**, 3375–3380
5 Kliewer, S. A., Moore, J. T., Wade, L., Staudinger, J. L., Watson, M. A., Jones, S. A., McKee, D. D., Oliver, B. B., Willson, T. M., Zetterstrom, R. H. et al. (1998) An orphan nuclear receptor activated by pregnanes defines a novel steroid signaling pathway. Cell **92**, 73–82
6 Bertilsson, G., Heidrich, J., Svensson, K., Asman, M., Jendeberg, L., Sydow-Backman, M., Ohlsson, R., Postlind, H., Blomquist, P. and Berkenstam, A. (1998) Identification of a human nuclear receptor defines a new signaling pathway for CYP3A induction. Proc. Natl. Acad. Sci. U.S.A. **95**, 12208–12213
7 Synold, T. W., Dussault, I. and Forman, B. M. (2001) The orphan nuclear receptor SXR coordinately regulates drug metabolism and efflux. Nat. Med. **7**, 584–590
8 Jeong, H., Choi, S., Song, J. W., Chen, H. and Fischer, J. H. (2008) Regulation of UDP-glucuronosyltransferase (UGT) 1A1 by progesterone and its impact on labetalol elimination. Xenobiotica **38**, 62–75
9 Lichti-Kaiser, K., Brobst, D., Xu, C. and Staudinger, J. L. (2009) A systematic analysis of predicted phosphorylation sites within the human pregnane X receptor protein. J. Pharmacol. Exp. Ther. **331**, 65–76

[2] http://www.ebi.ac.uk/s4/jump?from=aHR0cDovL3d3dy5lYmkuYWMudWsvczQvc3VtbWFyeS9tb2xlY3VsYXIvZXhwcmVzc2lvbj90ZXJtPXVicjUmY2xhc3NpZmljYXRpb249OTYwNiZ0aWQ9bmFtZU9yZ0VOU01VU0cwMDAwMDAzNzQ4Nw%3D%3D&hash=14B06&url=http://www.ebi.ac.uk/gxa/das/../gene/ENSG00000104517

[3] http://www.ebi.ac.uk/s4/jump?from=aHR0cDovL3d3dy5lYmkuYWMudWsvczQvc3VtbWFyeS9tb2xlY3VsYXIvZXhwcmVzc2lvbj90ZXJtPWR5cmsyJmNsYXNzaWZpY2F0aW9uPTk2MDYmdGlkPW5hbWVPcmdFTlNHMDAwMDAxMjczMzQ%3D&hash=30625&url=http://www.ebi.ac.uk/gxa/das/../gene/ENSG00000127334

10 Rana, R., Coulter, S., Kinyamu, H. and Goldstein, J. A. (2012) RBCK1, an E3 ubiquitin lLigase, interacts with and ubiquinates the human pregnane X receptor (hPXR). Drug Metab. Dispos. **41**, 398–405

11 Staudinger, J. L., Xu, C., Biswas, A. and Mani, S. (2011) Post-translational modification of pregnane X receptor. Pharmacol. Res. **64**, 4–10

12 Pondugula, S. R., Dong, H. and Chen, T. (2009) Phosphorylation and protein–protein interactions in PXR-mediated CYP3A repression. Expert Opin. Drug Metab. Toxicol. **5**, 861–873

13 Pondugula, S. R., Brimer-Cline, C., Wu, J., Schuetz, E. G., Tyagi, R. K. and Chen, T. (2009) A phosphomimetic mutation at threonine-57 abolishes transactivation activity and alters nuclear localization pattern of human pregnane x receptor. Drug Metab. Dispos. **37**, 719–730

14 Sugatani, J., Uchida, T., Kurosawa, M., Yamaguchi, M., Yamazaki, Y., Ikari, A. and Miwa, M. (2012) Regulation of pregnane X receptor (PXR) function and *UGT1A1* gene expression by posttranslational modification of PXR protein. Drug Metab. Dispos. **40**, 2031–2040

15 Hoeller, D., Hecker, C. M. and Dikic, I. (2006) Ubiquitin and ubiquitin-like proteins in cancer pathogenesis. Nat. Rev. Cancer **6**, 776–788

16 Masuyama, H., Hiramatsu, Y., Mizutani, Y., Inoshita, H. and Kudo, T. (2001) The expression of pregnane X receptor and its target gene, cytochrome P450 3A1, in perinatal mouse. Mol. Cell. Endocrinol. **172**, 47–56

17 Masuyama, H., Inoshita, H., Hiramatsu, Y. and Kudo, T. (2002) Ligands have various potential effects on the degradation of pregnane X receptor by proteasome. Endocrinology **143**, 55–61

18 Gwack, Y., Sharma, S., Nardone, J., Tanasa, B., Iuga, A., Srikanth, S., Okamura, H., Bolton, D., Feske, S., Hogan, P. G. and Rao, A. (2006) A genome-wide *Drosophila* RNAi screen identifies DYRK-family kinases as regulators of NFAT. Nature **441**, 646–650

19 Lin, W., Wu, J., Dong, H., Bouck, D., Zeng, F. Y. and Chen, T. (2008) Cyclin-dependent kinase 2 negatively regulates human pregnane X receptor-mediated *CYP3A4* gene expression in HepG2 liver carcinoma cells. J. Biol. Chem. **283**, 30650–30657

20 Wang, Y. M., Lin, W., Chai, S. C., Wu, J., Ong, S. S., Schuetz, E. G. and Chen, T. (2013) Piperine activates human pregnane X receptor to induce the expression of cytochrome P450 3A4 and multidrug resistance protein 1. Toxicol. Appl. Pharmacol. **272**, 96–107

21 Goktug, A. N., Ong, S. S. and Chen, T. (2012) GUItars: a GUI tool for analysis of high-throughput RNA interference screening data. PLoS One **7**, e49386

22 Zhang, X. D. (2011) Illustration of SSMD, z score, SSMD*, z* score, and t statistic for hit selection in RNAi high-throughput screens. J. Biomol. Screen **16**, 775–785

23 Zhang, X. D. (2007) A new method with flexible and balanced control of false negatives and false positives for hit selection in RNA interference high-throughput screening assays. J. Biomol. Screen **12**, 645–655

24 Zhang, X. D., Yang, X. C., Chung, N., Gates, A., Stec, E., Kunapuli, P., Holder, D. J., Ferrer, M. and Espeseth, A. S. (2006) Robust statistical methods for hit selection in RNA interference high-throughput screening experiments. Pharmacogenomics **7**, 299–309

25 Perkins, D. N., Pappin, D. J., Creasy, D. M. and Cottrell, J. S. (1999) Probability-based protein identification by searching sequence databases using mass spectrometry data. Electrophoresis **20**, 3551–3567

26 Dong, H., Lin, W., Wu, J. and Chen, T. (2010) Flavonoids activate pregnane x receptor-mediated CYP3A4 gene expression by inhibiting cyclin-dependent kinases in HepG2 liver carcinoma cells. BMC Biochem. **11**, 23

27 Sugatani, J., Osabe, M., Kurosawa, M., Kitamura, N., Ikari, A. and Miwa, M. (2010) Induction of UGT1A1 and CYP2B6 by an antimitogenic factor in HepG2 cells is mediated through suppression of cyclin-dependent kinase 2 activity: cell cycle-dependent expression. Drug Metab. Dispos. **38**, 177–186

28 Maddika, S. and Chen, J. (2009) Protein kinase DYRK2 is a scaffold that facilitates assembly of an E3 ligase. Nat. Cell Biol. **11**, 409–419

29 He, Y. J., McCall, C. M., Hu, J., Zeng, Y. and Xiong, Y. (2006) DDB1 functions as a linker to recruit receptor WD40 proteins to CUL4–ROC1 ubiquitin ligases. Genes Dev. **20**, 2949–2954

30 Johnson, D. R., Li, C. W., Chen, L. Y., Ghosh, J. C. and Chen, J. D. (2006) Regulation and binding of pregnane X receptor by nuclear receptor corepressor silencing mediator of retinoid and thyroid hormone receptors (SMRT). Mol. Pharmacol. **69**, 99–108

31 Raynal, C., Pascussi, J. M., Leguelinel, G., Breuker, C., Kantar, J., Lallemant, B., Poujol, S., Bonnans, C., Joubert, D., Hollande, F. et al. (2010) Pregnane X Receptor (PXR) expression in colorectal cancer cells restricts irinotecan chemosensitivity through enhanced SN-38 glucuronidation. Mol. Cancer **9**, 46

32 Noble, S. M., Carnahan, V. E., Moore, L. B., Luntz, T., Wang, H., Ittoop, O. R., Stimmel, J. B., Davis-Searles, P. R., Watkins, R. E., Wisely, G. B. et al. (2006) Human PXR forms a tryptophan zipper-mediated homodimer. Biochemistry **45**, 8579–8589

33 Stirnimann, C. U., Petsalaki, E., Russell, R. B. and Muller, C. W. (2010) WD40 proteins propel cellular networks. Trends Biochem. Sci. **35**, 565–574

34 Campbell, L. E. and Proud, C. G. (2002) Differing substrate specificities of members of the DYRK family of arginine-directed protein kinases. FEBS Lett. **510**, 31–36

35 Clancy, J. L., Henderson, M. J., Russell, A. J., Anderson, D. W., Bova, R. J., Campbell, I. G., Choong, D. Y., Macdonald, G. A., Mann, G. J., Nolan, T. et al. (2003) EDD, the human orthologue of the hyperplastic discs tumour suppressor gene, is amplified and overexpressed in cancer. Oncogene **22**, 5070–5081

36 O'Brien, P. M., Davies, M. J., Scurry, J. P., Smith, A. N., Barton, C. A., Henderson, M. J., Saunders, D. N., Gloss, B. S., Patterson, K. I., Clancy, J. L. et al. (2008) The E3 ubiquitin ligase EDD is an adverse prognostic factor for serous epithelial ovarian cancer and modulates cisplatin resistance *in vitro*. Br. J. Cancer **98**, 1085–1093

37 Gorringe, K. L., Boussioutas, A. and Bowtell, D. D. (2005) Novel regions of chromosomal amplification at 6p21, 5p13, and 12q14 in gastric cancer identified by array comparative genomic hybridization. Genes Chromosomes Cancer **42**, 247–259

38 Miller, C. T., Aggarwal, S., Lin, T. K., Dagenais, S. L., Contreras, J. I., Orringer, M. B., Glover, T. W., Beer, D. G. and Lin, L. (2003) Amplification and overexpression of the dual-specificity tyrosine-(Y)-phosphorylation regulated kinase 2 (*DYRK2*) gene in esophageal and lung adenocarcinomas. Cancer Res. **63**, 4136–4143

Received 19 April 2013/17 January 2014; accepted 20 January 2014
Published as BJ Immediate Publication 20 January 2014, doi:10.1042/BJ20130558

Biochem. J. (2014) **459**, 193–203 (Printed in Great Britain) doi:10.1042/BJ20130558

online data

SUPPLEMENTARY ONLINE DATA

Stability of the human pregnane X receptor is regulated by E3 ligase UBR5 and serine/threonine kinase DYRK2

Su Sien ONG*, Asli N. GOKTUG*, Ayesha ELIAS*, Jing WU*, Darren SAUNDERS† and Taosheng CHEN*[1]

*Department of Chemical Biology and Therapeutics, St. Jude Children's Research Hospital, 262 Danny Thomas Place, Memphis, TN 38105, U.S.A.
†Cancer Research Program, Garvan Institute of Medical Research, 384 Victoria Street, Darlinghurst NSW 2010, Australia

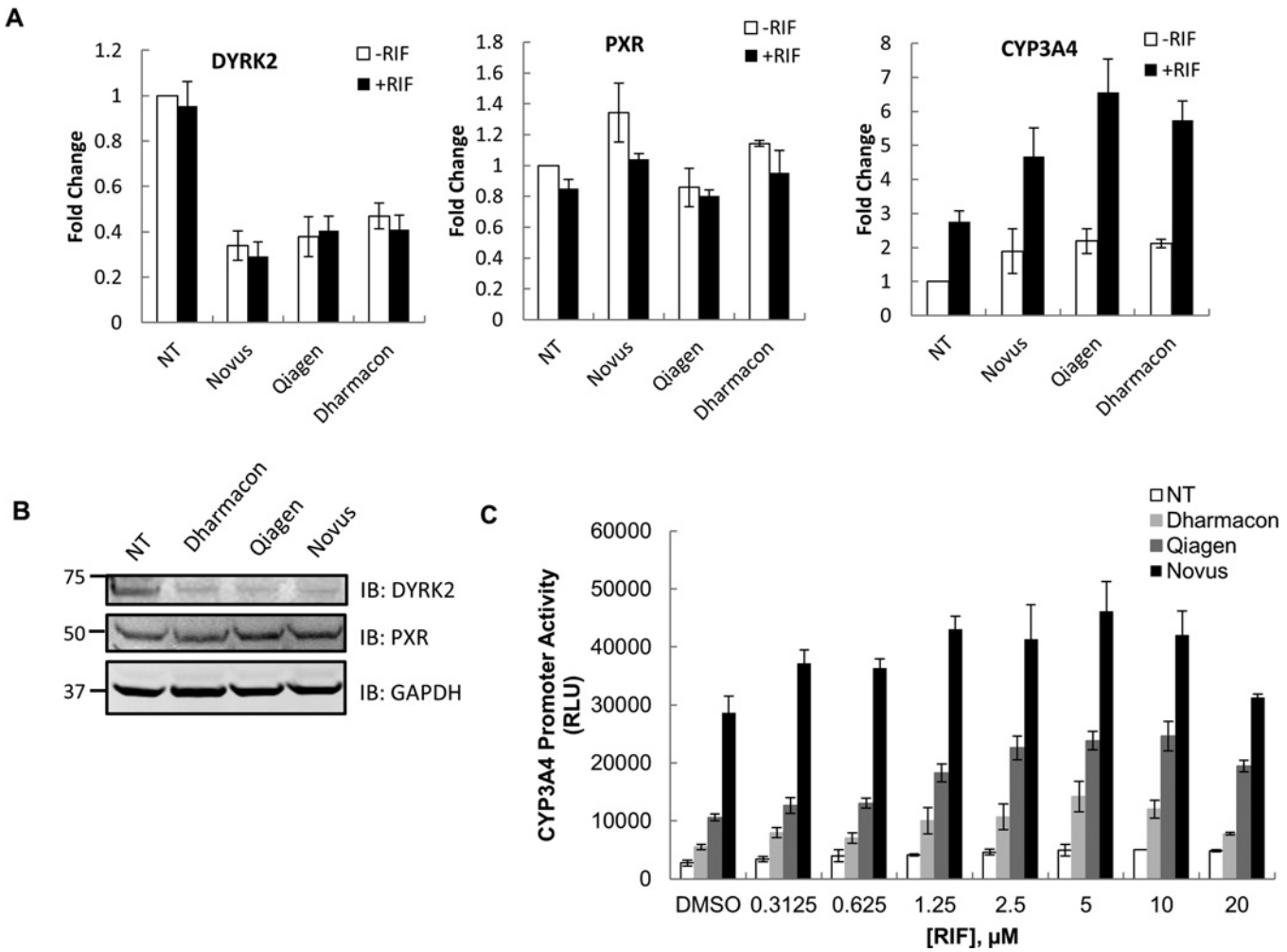

Figure S1 DYRK2 knockdown does not affect hPXR transcript level

(**A**) RT–PCR was performed to determine the transcript level of DYRK2 (left-hand panel), hPXR (middle panel) and CYP3A4 (right-hand panel) after a 24 h treatment with DMSO (− RIF) or 5 μM rifampicin (+ RIF) in HepG2 cells stably expressing CYP3A4-luc and transiently transfected with either non-targeting siRNA (NT) or siDYRK2 obtained from various sources as indicated. The value from untreated (− RIF) non-targeting siRNA was set as 1. (**B**) siRNA knockdown of DYRK2 was performed on HepG2 cells. At 72 h post-transfections, cells were harvested and prepared for Western blot analysis (IB) using antibodies as indicated. (**C**) Dose–response of rifampicin in activating CYP3A4-luc in HepG2 cells stably expressing CYP3A4-luc and transiently transfected with either non-targeting shRNA or siDYRK2.

Received 19 April 2013/17 January 2014; accepted 20 January 2014
Published as BJ Immediate Publication 20 January 2014, doi:10.1042/BJ20130558

[1] To whom correspondence should be addressed (email taosheng.chen@stjude.org).